



ELSEVIER

Journal of Photochemistry and Photobiology A: Chemistry 142 (2001) 169–175

Journal of
Photochemistry
and
Photobiology
A: Chemistry

www.elsevier.com/locate/jphotochem

Time-resolved fluorescence imaging of photosensitiser distributions in mammalian cells using a picosecond laser line-scanning microscope

James P. Connelly^a, Stanley W. Botchway^b, Lars Kunz^a,
David Pattison^a, Anthony W. Parker^b, Alexander J. MacRobert^{a,*}

^a National Medical Laser Centre, Royal Free and University College Medical School, University College London,
67-73 Riding House Street, Charles Bell House, London W1W 7EJ, UK

^b Lasers for Science Facility, Rutherford Appleton Laboratory, CLRC, Chilton, Oxon, UK

Abstract

A fluorescence microscope using line-excitation generated from a pulsed picosecond dye laser source has been combined with a gated sub-nanosecond high repetition rate (800 kHz) image intensifier to enable time-gated fluorescence lifetime imaging. Using this system, several potential photosensitisers for photodynamic therapy (PDT) have been studied. The fluorescence of the anionic disulphonated aluminium phthalocyanine (AlPcS₂) and cationic pyridinium zinc(II) phthalocyanine (ZnPPC) has been imaged in hamster V79-4 fibroblasts and compared with AlPcS₂ and *meta*-tetra(hydroxyphenyl) chlorin (*m*-THPC) in murine macrophages (J774A.1). Lifetime images were obtained from nanosecond delay sequences of fluorescence images with detector gate widths of 700 ps by fitting the data to single lifetime decays. AlPcS₂ and ZnPPC fluorescence appeared to be localised predominantly in perinuclear sites and absent from the nucleus. Similar regional average lifetime ranges in both cell lines for AlPcS₂ were observed, varying between 4 and 5 ns at the most intense sites of fluorescence. ZnPPC exhibited more uniform lifetime maps with average lifetimes of 2.5–3.0 ns. The chlorin *m*-THPC fluorescence was also extranuclear and appeared more homogeneously distributed, but was strongly affected by photobleaching. This study demonstrates the utility of the laser line-scanning technique for rapid acquisition of time-gated fluorescence lifetime images. © 2001 Elsevier Science B.V. All rights reserved.

Keywords: Fluorescence lifetime imaging; Fluorescence microscopy; Phthalocyanine; Photodynamic therapy; PDT

1. Introduction

The treatment of certain malignant and benign lesions using photosensitising drugs is gaining increasing clinical interest [1–3]. Photodynamic therapy (PDT), as it is termed, consists of administration of a light-activated drug (photosensitiser), or prodrug, followed by illumination. Selective tumour destruction is obtained by fibre-optic delivery of the light and, in the case of some photosensitisers, improved by tumour retention of the drug. In the treatment of slower growing skin cancers, such as basal cell carcinoma [4], the use of topical application and excellent cosmetic outcome

have established PDT as a strong competitor to other current methods of treatment. The simplicity of PDT however, belies a complexity ranging from cell metabolism to tissue optics. To harness the full potential of PDT, photosensitiser properties and pharmacokinetics in cells and tissues need to be characterised to further understanding of PDT processes, improve dosing and develop new strategies [5]. Fluorescence detection of photosensitisers is the most sensitive means of measuring cell and tissue distributions, however the effects of intracellular microenvironmental factors and aggregation which could lead to fluorescence quenching remain largely unquantified.

A fluorescence microscope system has been developed which enables rapid, low laser power, time-resolved fluorescence imaging with the capability of confocal resolution. This technique has been applied to the study of the fluorescence lifetime dynamics of PDT photosensitisers in cells and tissues [6]. Since exposure to light initiates photochemical reactions as well as fluorescence of the photosensitiser, low light intensity and rapid measurement time are crucial. To optimise imaging speed, a line-scanning microscope

Abbreviations: AlPcS₂, disulphonated aluminium phthalocyanine; CCD, charge-coupled device; CLSM, confocal laser scanning microscope; FCS, foetal calf serum; GOI, gated optical intensifier; HRI, high-rate intensifier; *m*-THPC, *meta*-tetra(hydroxyphenyl) chlorin; PBS, phosphate-buffered saline; PDT, photodynamic therapy; ZnPPC, pyridinium zinc(II) phthalocyanine

*Corresponding author. Tel.: +44-207-679-9838;
fax: +44-207-813-2828.

E-mail address: a.macrobert@ucl.ac.uk (A.J. MacRobert).

with a sensitive charge-coupled device (CCD) has been employed [7,8] which has been enhanced by the addition of a high-rate (800 kHz) sub-nanosecond-gated and intensified imaging detector. This configuration enables time-resolved fluorescence microscopy and the extra dimension of lifetime imaging [9,10]. The latter gives information about the environment of the fluorescing probe and can distinguish spectrally overlapping molecules by their lifetimes [11]. With rapid line-scanning microscopy which yields both fluorescence intensity and lifetime data, we have been able to study photosensitiser localisation and environment, and the changes accompanying PDT and photobleaching.

Using confocal laser scanning microscopy (CLSM) and co-staining with lipid-probe Nile Red, we have previously shown that in Chinese hamster V79-4 fibroblasts, zinc and aluminium phthalocyanines localise in perinuclear sites [10]. These sites were disrupted by PDT and fluorescence redistribution was observed. We extended this study and present here fluorescence lifetime images of the ionic photosensitisers, anionic disulphonated aluminium phthalocyanine (AlPcS₂) and cationic pyridinium zinc(II) phthalocyanine (ZnPc) [12] in Chinese hamster V79-4 fibroblasts and murine (J774A.1) macrophages. We have compared these results with *meta*-tetra(hydroxyphenyl) chlorin (*m*-THPC) (Foscan[®]), a hydrophobic and uncharged photosensitiser, and considered the effects of PDT and photobleaching.

2. Materials and methods

2.1. Apparatus

The fluorescence microscope employed in this study is a combination of the line-scanning confocal fluorescence microscope [7] and time-resolved fluorescence microscope [10] systems developed previously for photosensitiser imaging. A schematic diagram of the apparatus is shown in Fig. 1. A picosecond laser system was employed consisting of a cavity-dumped dye laser (Spectra Physics, model 3500) pumped synchronously by a mode-locked Nd³⁺/YAG laser (Spectron, model SL903). The duration of the dye laser pulses was approximately 6 ps and the excitation wavelengths used in this work were 610 nm for AlPcS₂ and 590 nm for *m*-THPC. The average laser excitation power was about 6 μW during image acquisition to minimise photobleaching of the intracellular photosensitiser fluorescence. An inverted microscope (Olympus, IMT-2) was used and the fluorescence images were obtained using a 63× objective (Nikon PlanAchromat, 1.4 NA). For the line-scanning, the laser excitation beam was focused to a vertical line and collimated into an expanded beam which was transmitted through a dichroic mirror (DM) (Fig. 1, Omega Optical, 630DCSP) and scanned using a double-sided scanning mirror (SM, General Scanning, M3H) to reflect the laser line into the microscope. The optics of the microscope were used to direct

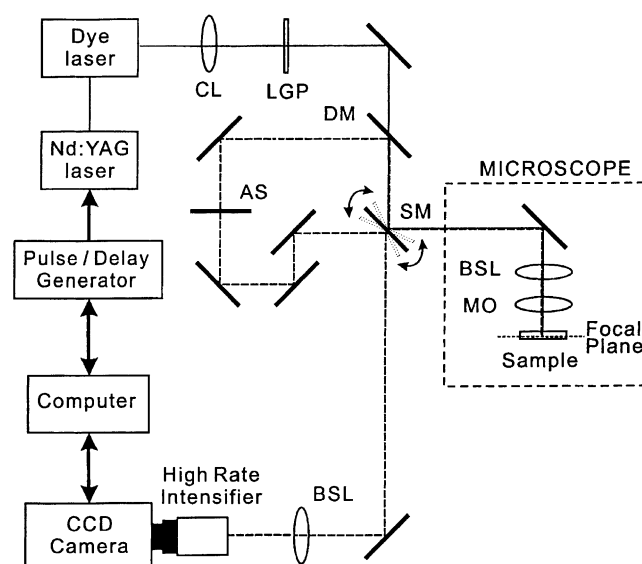


Fig. 1. Schematic diagram of the time-resolved line-scanning laser confocal microscope. Solid line: the excitation beam; dashed line: the emission beam; arrows: data communication. Abbreviations: CL, cylindrical lens; LGP, line-generation plane; DM, dichroic mirror; SM, scanning mirror; BSL, beam steering lens; MO, microscope objective; AS, adjustable slit.

and focus the beam into the sample and the emitted fluorescence (dashed line) was collected by the same objective and focused on to the semi-reflective scanning mirror. An adjustable slit (AS) allowed control of the depth of focus so that with samples that were sufficiently fluorescent, the apparatus could be operated confocally. Excitation and emission light were separated using dichroic mirrors allowing projection of an image of the slit on to the two-dimensional detector. Any extraneous scattered excitation light was further attenuated using a long-pass filter (Schott, RG630) placed in front of the gated optical detector. Using this configuration with a narrow-slit setting, it was possible to achieve confocal imaging with an optimal axial resolution of 2 μm determined by calibration using fluorescent spheres (Molecular Probes, F-8826), whilst the lateral resolution was less than 1 μm measured with a graticule. In practice however, wider slits have to be used in order to obtain useable signal intensities. Images were collected on an 8 bit scientific grade CCD camera capable of on-chip integration (Cohu, 4910). The bilateral scanning mirror was made to oscillate at 25 Hz by a sawtooth signal supplied by a function generator (Thandar, TG501) to match the video frame rate of the CCD camera. This resulted in two complete scans of the laser excitation line across the microscope field per video frame, yielding real-time fluorescence images on the video monitor for samples that were sufficiently fluorescent. All images presented in this work were recorded by integrating for up to 4 s (100 video frames) on the CCD chip.

The gated high-rate intensifier (HRI, Kentech Instruments Ltd., UK) was operated at 800 kHz to match the pulse repetition rate of the dye laser. A sync signal from the laser cavity dumper driver was used to trigger the digital

pulse/delay generator (Kentech Instruments Ltd., UK) allowing sub-nanosecond delay control of the HRI gate, with jitter of about 40 ps. A gate width of 700 ps was used for all time-gated imaging measurements. The first gate was positioned by adjusting the delay until maximum gated fluorescence was obtained and taken to correspond to zero delay. This correlated with the leading edge of the gate coinciding with the laser pulse, as judged by comparing the output from the gate controller with a fast laser diode positioned at the detector.

Intracellular fluorescence spectra from macrophages were recorded at 1 nm resolution using the inverted microscope coupled to 0.125 m focal length spectrograph (Multispec, LOT-Oriel Ltd., UK) with 600 lines/mm diffraction grating and a Peltier cooled CCD camera (Mark II, Wright Instruments Ltd., UK). Fluorescence was excited using blue light (380–450 nm) generated by an Xe-arc lamp (PX-1, Ocean Optics Inc., US, optical output < 1 mW after filtering), directed through a condenser into the dichroic mirror housing of the microscope for conventional epifluorescence excitation. A long-pass filter was placed before the CCD camera to remove any transmitted excitation light. Spectra were acquired with 10 s integration without any photo-induced changes.

2.1.1. Sample preparation and cell culture

Sulphonated metal phthalocyanines (AlPcS₂) were prepared according to the method of Ambroz et al. [13]. ZnPPC was provided by Prof. S. Brown, Leed University [12] and *m*-THPC by Scotia Quantanova, UK. Chinese hamster V79-4 lung fibroblasts were prepared as described previously [7]. Murine macrophages (J774A.1, ECACC, Centre of Applied Microbiology and Research, UK) were cultured in DMEM containing 10% foetal calf serum (FCS) (phenol red-free, supplemented with 1% L-glutamine and 1% penicillin and streptomycin) at 37°C under humidified air with 5% CO₂. Cells were incubated (in the absence of serum) with either 20 or 100 μM AlPcS₂ for 1–3 h or 10–50 μM ZnPPC for 1 h or 15 μM *m*-THPC and 2% FCS for 24 h at 37°C. This was followed by thorough washing with phosphate-buffered saline (PBS) prior to measurements.

2.1.2. Fluorescence lifetime analysis

Fluorescence lifetimes were calculated from sets of five or six images collected over 0–4 ns in 1 ns step delays for AlPcS₂, or over 0–10 ns in 2 ns steps for *m*-THPC, following arrival of the excitation pulse at the sample. Intracellular fluorescence lifetime images were analysed using C++ routines allowing single exponential decay fits using the formula:

$$\ln [D_t(x, y)] = \ln B(x, y) - \frac{t}{\tau(x, y)} \quad (1)$$

as described in previous lifetime studies [10]. Averaged area (10 × 10 pixel square) point decays were also analysed using standard exponential fitting routines in Sigmaplot.

3. Results

Calibration measurements of AlPcS₂ (20 μM) in thin films of aqueous solution on a microscope slide gave an average lifetime of 4.8 ± 0.7 ns in good agreement with previously reported values [10]. In V79 cells incubated with AlPcS₂, all fluorescence images, regardless of concentration or incubation time, showed highest fluorescence in the perinuclear region and less in the cell membrane, as illustrated in Fig. 2a and b. Fluorescence was largely absent in the nucleus. Despite the variable fluorescence intensity, lifetimes were quite homogeneously distributed, as shown in Fig. 2c.

The intracellular decay of AlPcS₂ fluorescence (averaged over 10 × 10 pixels), incubated at a higher concentration (100 μM) than our previous studies, was measured in the most intense fluorescent region. A good fit was given by a single exponential, as shown in Fig. 3a, and a mean lifetime of 4.8 ± 0.3 ns was obtained. However, histograms of the AlPcS₂ lifetime distribution in cells (an example given in Fig. 3b) obtained using the lifetime imaging software were notably broader than in solution. Similar results were obtained using 20 μM concentrations.

The time-gated fluorescence images of V79-4 cells treated with ZnPPC were similar to AlPcS₂ and showed perinuclear localisation. The lifetime maps exhibited little variation over the cell between bright and dark areas, with an average lifetime of 2.5–3.0 ns. The incubation conditions were varied with concentrations from 10–50 μM ZnPPC, but with little change in the measured lifetimes.

For comparison, *m*-THPC or AlPcS₂ uptake in macrophages was investigated. Since macrophages are known to accumulate high levels of photosensitisers in vitro (and in vivo), we hoped to obtain much higher fluorescence intensities which would have enabled higher resolution imaging. However, there was little improvement over the V79 cell line, most likely due to aggregation of the fluorescent monomeric moiety to weakly or non-fluorescent dimers and higher aggregates. Overall, the distribution and lifetime (mean value 4.0 ± 0.2 ns) of AlPcS₂ (100 μM) in macrophages appeared similar to those in V79 cells. Cells incubated with *m*-THPC for 24 h showed a more uniformly distributed fluorescence within the cell than with AlPcS₂. There was little fluorescence evident in the nucleus. Calibration of *m*-THPC (15 μM) in methanol gave a lifetime of 8 ± 0.4 ns. Single lifetime analysis of the cellular images gave very broad lifetime distribution histograms with modal lifetime values around 5.0 ns, although photobleaching was difficult to minimise. In contrast, using AlPcS₂, incubation of cells for a longer period of time or with higher concentrations appeared to result in a fluorescence intensity increase and redistribution during irradiation, as reported previously by Scully et al. [7] using the V79 cell line. However, no fluorescence increase was observed in the case of *m*-THPC. We attempted to measure any changes in AlPcS₂ lifetime distributions induced by irradiation (both during and after), but were thwarted by

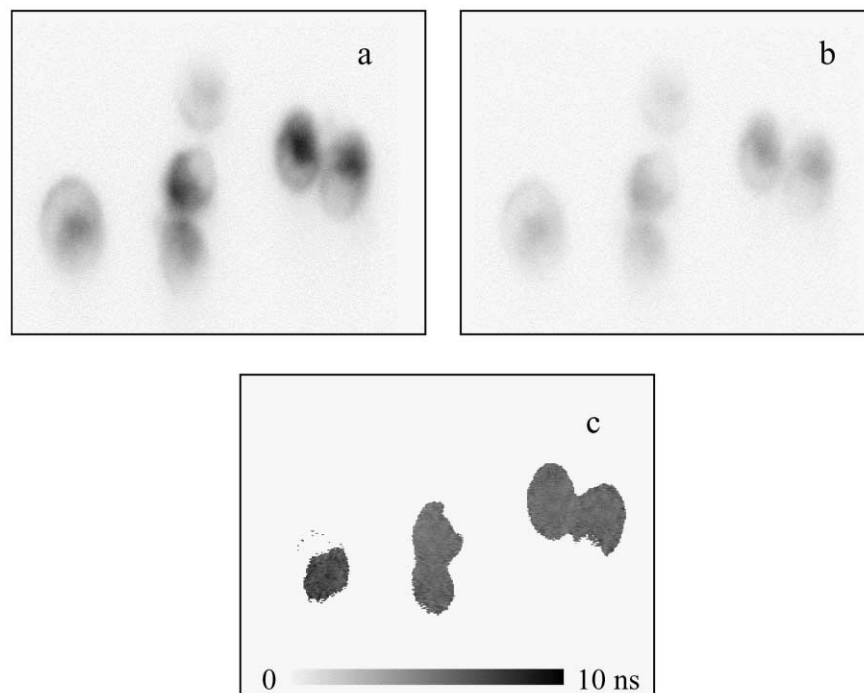


Fig. 2. Images of V79 cells incubated with $100 \mu\text{M}$ AlPcS₂ for 2 h, with image widths of $110 \mu\text{m}$: (a) gated fluorescence image at laser pulse; (b) gated image 4 ns after laser pulse; (c) fluorescence lifetime map of five gated images including images (a) and (b).

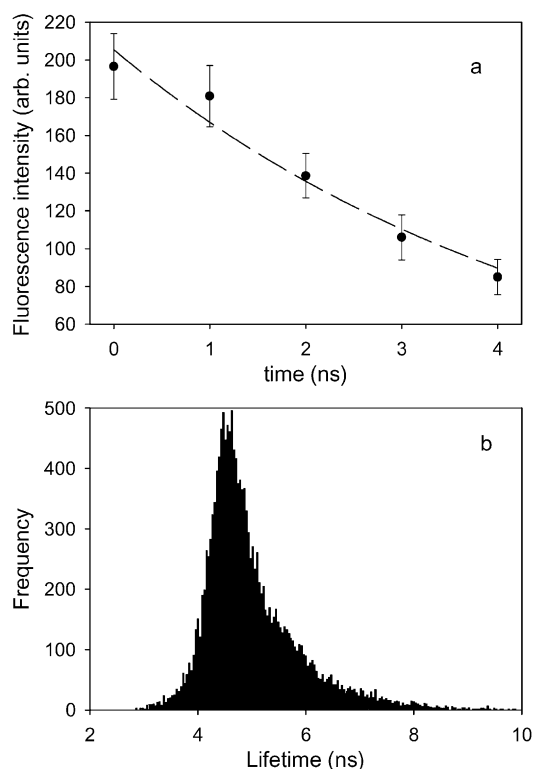


Fig. 3. Lifetime analysis of V79 cells incubated with $100 \mu\text{M}$ AlPcS₂ for 2 h (imaged in Fig. 2): (a) non-linear single exponential fit (dashed line) of an averaged 10×10 pixel area in a highly fluorescing region of five gated and delayed fluorescence images; error bars indicate the standard deviation and average lifetime is 4.8 ± 0.3 ns; (b) lifetime histogram of the V79 cell lifetime map shown in Fig. 2c.

fluorescence redistribution and increase following prolonged irradiation.

The light-induced increase in fluorescence intensity is illustrated in Fig. 4 which shows microspectrofluorimetric spectra with peak emission at 682 nm recorded from a microscopic field containing up to 10 cells (macrophages) using irradiation at 670 nm; the irradiation power was significantly larger ($>10 \text{ mW/cm}^2$) than used for the lifetime measurements, and the fluorescence excitation intensity

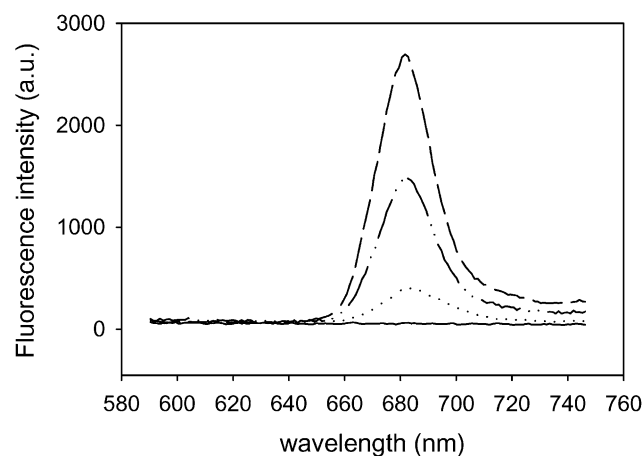


Fig. 4. Microfluorimetric emission spectra of macrophages incubated with $10 \mu\text{M}$ AlPcS₂ for 18 h after washing with PBS. Solid line: background without cells; dotted line: fluorescence before PDT; dashed line: fluorescence after 1 min of irradiation at 670 nm and 75 mW/cm^2 to initiate PDT, followed by 15 min in the dark; dot and dash line: fluorescence after further irradiation for 10 min.

from the Xe lamp was too small to induce any perturbations. After a short period of irradiation of 1 min, the spectral intensity increases without any apparent alteration in the spectral profile; we also found that the increase continued after the laser irradiation had ended which is the subject of further study. With a longer period of irradiation, a decline in intensity was observed due to photobleaching of the phthalocyanine [7].

4. Discussion

A tuneable time-resolved line-scanning laser fluorescence microscope with a sub-nanosecond-gated high repetition rate optical image detector with confocal capability has been developed for fluorescence lifetime imaging. Line-scanning enables far more rapid image acquisition than the more conventional point scanning system, requiring only one lateral scan across the field to capture one image frame on the imaging detector. Although, this leads to a reduction in axial resolution, the resolution is still better than with a conventional fluorescence microscope [8] and photobleaching effects, that can hinder lifetime measurements in a point scanning system, are reduced. To improve our earlier gated detection system [9,10], we replaced the 8 kHz gated optical intensifier (GOI) with an HRI version. The latter can be operated to match the laser pulse frequency (800 kHz), allowing faster data integration and lower laser power. The peak-to-peak jitter of the HRI is less than 40 ps, and the minimum gate width is 300 ps. Since the lifetime measurement is not directly dependent on the gate width, many biomolecular probes with sub-nanosecond lifetimes can potentially be investigated [9]. The HRI also improved the spatial resolution compared to the GOI system.

Previously, we have shown using lower concentrations of AlPcS₂ (10 μM for 1 h or less) than used in this study, that the fluorescence is localised within perinuclear sites, probably comprising the Golgi apparatus, the endoplasmic reticulum and lysosomes rather than mitochondria [7,10]. A study by Moan et al. [14] reports that with longer incubation times (18 h), a granular fluorescence distribution, corresponding with localisation in the lysosomes, is observed. In this study, we find a more general fluorescence distribution analogous to the former study, even at high concentration and 3 h incubation. The fluorescence lifetime maps obtained do not show any clear correlation with the intracellular fluorescence intensity distribution (for example see Fig. 2a and c). This suggests that although non-uniformly distributed throughout the cell, the fluorescing AlPcS₂ is largely in the same type of microenvironment. The increase in AlPcS₂ fluorescence observed in the cells on irradiation, as illustrated in Fig. 4, and subsequent redistribution has been attributed to photodynamically induced disruption of membranes and the release and disaggregation of AlPcS₂ to monomers with a much higher fluorescence quantum yield from membrane structures (e.g. lysosomes) [7,15].

The range of AlPcS₂ lifetimes observed in this study is broader and tends towards values shorter than those found for AlPcS₂ in water ($\tau = 5$ ns), bound to protein ($\tau = 5.5$ ns) or in methanol ($\tau = 6.1$ ns) [16], as illustrated in Fig. 3b. Although, the longer lifetimes correlate with the lowest fluorescence regions at the cell edges, and probably reflect the noise offset extending the lifetime, the spread to shorter lifetimes in cells however suggests environmental effects or increased fluorescence quenching [17]. This may reflect a concentration effect on AlPcS₂ fluorescence lifetimes analogous to the effect reported in liposomal solutions of small or large unilamellar vesicles. In that study, a histogram analysis of lifetime distributions found that the modal lifetime became shorter and tended towards 4 ns with increasing AlPcS₂ concentration [18]. A much shorter lifetime component (<1 ns) with a lower amplitude was also observed. At low AlPcS₂ concentrations, the lifetime distribution was relatively narrow with a modal value of 6.8 ns. The reduction in fluorescence lifetime at higher concentrations was attributed to fluorescence quenching of monomers via energy transfer to non-fluorescent aggregates which have a broad absorption band overlapping the monomeric fluorescence emission spectrum. In this study, we have used a relatively high concentration of AlPcS₂ (100 μM for 2 h) compared to previous studies [10] (10 μM for 1 h or less) in order to establish whether the lifetime dynamics are affected by the intracellular concentration and the degree of sensitiser aggregation. Although, this study was statistically too small to show any detailed correlations, it is apparent that there are no gross differences in the intracellular lifetimes in either the fibroblast V79 or macrophage cell lines at the higher AlPcS₂ concentrations. Using the lower concentrations investigated previously [10], a monoexponential fit gave 4.0 ns, although a biexponential decay was found to give a slightly better fit with 1.1 and 5.4 ns. In the present study using the higher concentration conditions, a histogram of the lifetime distribution revealed a range of lifetimes from about 3 to 7 ns with a modal value of about 4.3 ns. Overall, it appears that the intracellular lifetime distributions correlate remarkably well with those observed in liposomal model systems for which at higher concentrations, the AlPcS₂ is aggregated (as shown from absorbance spectra) and a shortening of the fluorescence lifetime to near 4 ns and a much lower fluorescence quantum yield were observed. The photo-induced intracellular fluorescence redistribution and intensity increase following irradiation is consistent with the proposal that the AlPcS₂ is strongly aggregated in the cells prior to irradiation. The increase in fluorescence intensity is primarily due to sensitiser disaggregation to fluorescent monomers resulting from photo-induced rupture of organelle structures. The dilution of the aggregate concentration also reduces the degree of fluorescence quenching (via energy transfer to aggregates), but this would be a secondary factor contributing to the fluorescence increase.

The studies with the cationic ZnPPC sensitiser were in many respects similar to that of the anionic AlPcS₂. Pre-

vious studies of ZnPPC in RIF-1 murine sarcoma cells by steady-state fluorescence microscopy showed that ZnPPC localises predominantly in lysosomes, with extensive relocalisation following exposure to light [12]. The ZnPPC lifetime in the V79 cells was shorter than AlPcS₂ in the range of 2.5–3.0 ns (over 10–50 μ M) which is probably due to an enhanced rate of intersystem crossing with the heavier central Zn, by analogy with lifetime data for ZnPc and ClAlPc. With better imaging sensitivity, it may be possible to refine these conclusions, but the intracellular redistribution and intensity increase effects inherently limit signal integration times and thus the precision of the lifetime fits. In case of *m*-THPC, photobleaching was a more severe problem than with the phthalocyanines. In the macrophage cell line, *m*-THPC shows a similar but more uniform cellular fluorescence distribution to AlPcS₂ which may reflect differences in the uptake mechanism of the photosensitisers. In this study, *m*-THPC is dissolved in the medium by addition of 2% FCS which also mediates cellular uptake of *m*-THPC. In cells, *m*-THPC tends to localise generally in lipophilic environments [19], while less hydrophobic AlPcS₂, which is taken up by endocytosis, has a more restricted distribution [14]. Fluorescence decay measurements of *m*-THPC in vivo or dissolved in ethanol have been reported to give single exponential decay lifetimes of between 8.5 and 10.0 ns, respectively [20]. Measurements of *m*-THPC in methanol using the microscope system gave a lifetime of 8 ns, and single lifetime analysis of the cellular images gave very broad lifetime distribution histograms with modal lifetime values around 5 ns. This is significantly shorter than the range of lifetimes reported elsewhere [20], and we conclude that despite the improvements in instrumental speed and sensitivity, photobleaching of *m*-THPC leads to inherent artifacts in lifetime analysis shortening the observed fluorescence lifetime.

In this report, we have investigated the potential of using time-resolved lifetime imaging of photosensitiser fluorescence to study intracellular photophysical properties. We have demonstrated the utility of combining line-scanning fluorescence microscopy with rapid sub-nanosecond time-resolved two-dimensional detection. By matching a higher duty cycle intensifier to the laser pulse frequency, a more efficient use of the laser system was achieved. Lower laser powers and faster image integration also reduced photobleaching effects. Using currently available intensifier technology, further improvements in time resolution would be possible, however this would be at the expense of signal intensity for fluorophores with nanosecond lifetimes. However, for relatively photostable fluorophores, unlike photosensitisers, this should be readily achieved using longer acquisition times and could be extended to multiexponential lifetime imaging.

The microscope scanning system in this study incorporated an adjustable slit that confers confocal operation with a suitably photostable fluorophore [7,8]. The slit-scanning method may also be adapted for two-photon excitation

[21] and potentially multiphoton confocal lifetime imaging. The use of multiphoton excitation is preferable where photobleaching is a major problem, since this technique results in much less bleaching in planes above and below where the laser is focused [22,23]. An alternative confocal system using similar laser and gating technology together with structured illumination generated using a grid has been recently reported by Cole et al. [24]. Yet another approach is to use frequency rather than time domain methods and significant progress is being made with this alternative technique [6]. In the longer term with recent developments of compact ultrafast pulsed diode lasers, practical and portable real-time fluorescence lifetime imaging will be achievable for both microscopic and even clinical use.

Acknowledgements

This article is presented as a dedication to Lord Porter and we would like to acknowledge his interest in the idea of using phthalocyanine compounds for PDT which was developed by Prof. David Phillips at The Royal Institution. We are also grateful to Prof. S.B. Brown and Dr. D. Vernon (University of Leeds) for their kind contribution of the ZnPPC. Lars Kunz would like to thank the German Academic Exchange Service (Deutscher Akademischer Austauschdienst, Gemeinsames Hochschulsonderprogramm III) for a post-doctoral fellowship. We wish to thank Kentech for the provision of the HRI, Mrs. C. de Lara (RAGSU, MRC, UK) for providing V79 Chinese hamster fibroblast cultures, Drs. M. Towrie, P. Matausek and K. Henbest for assistance with the lasers, and Zdenek Petrusek for assistance with the analysis programs. The *m*-THPC was supplied as a gift from Scotia Pharmaceuticals Ltd. This project was supported by the BBSRC.

References

- [1] C. Hopper, *Lancet Oncol.* 1 (2000) 212.
- [2] R. Bonnett, *Rev. Contemporary Pharmacotherapy* 10 (1999) 1.
- [3] M. Ochsner, *Arzneimittel-Forschung-Drug Res.* 47 (1997) 1185.
- [4] V.C. Colussi, D.K. Feyes, H. Mukhtar, *Skin Pharmacol. Appl. Skin Physiol.* 11 (1998) 336.
- [5] D. Phillips, *Prog. React. Kinet.* 22 (1997) 175.
- [6] P.I.H. Bastiaens, A. Squire, *Trends Cell Biol.* 9 (1999) 48.
- [7] A.D. Scully, R.B. Ostler, A.J. MacRobert, A.W. Parker, C. de Lara, P. O'Neill, D. Phillips, *Photochem. Photobiol.* 68 (1998) 199.
- [8] G.J. Brakenhoff, K. Visscher, *J. Microsc. (Oxford)* 171 (1993) 17.
- [9] A.D. Scully, A.J. MacRobert, S. Botchway, P. O'Neill, A.W. Parker, R.B. Ostler, D. Phillips, *J. Fluoresc.* 6 (1996) 119.
- [10] A.D. Scully, R.B. Ostler, D. Phillips, P. O'Neill, K.M.S. Townsend, A.W. Parker, A.J. MacRobert, *Bioimaging* 5 (1997) 9.
- [11] K. Carlsson, A. Liljeborg, *J. Microsc. (Oxford)* 185 (1997) 37.
- [12] D.J. Ball, S. Mayhew, S.R. Wood, J. Griffiths, D.I. Vernon, S.B. Brown, *Photochem. Photobiol.* 69 (1999) 390.
- [13] M. Ambroz, A. Beeby, A.J. MacRobert, M.S.C. Simpson, R.K. Svensen, D. Phillips, *J. Photochem. Photobiol. B: Biol.* 9 (1991) 87.

- [14] J. Moan, K. Berg, H. Anholt, K. Madslien, *Int. J. Cancer* 58 (1994) 865.
- [15] Z. Petrusek, R.B. Ostler, I.V. Eigenbrot, D. Phillips, *SPIE Conf. Adv. Fluoresc. Sensing Technol. IV* 3602 (1999) 285.
- [16] M. Ambroz, A.J. MacRobert, J. Morgan, G. Rumbles, M.S.C. Foley, D. Phillips, *J. Photochem. Photobiol. B: Biol.* 22 (1994) 105.
- [17] R.F. Chen, J.R. Knutson, *Anal. Biochem.* 172 (1988) 61.
- [18] S. Dhami, G. Rumbles, A.J. MacRobert, D. Phillips, *Photochem. Photobiol.* 65 (1997) 85.
- [19] R. Hornung, B. Jentsch, N.E.A. Crompton, U. Haller, H. Walt, *Lasers Surgery Med.* 20 (1997) 443.
- [20] T. Glanzmann, J.P. Ballini, H. van den Bergh, G. Wagnieres, *Rev. Sci. Instrum.* 70 (1999) 4067.
- [21] G.J. Brakenhoff, J. Squier, T. Norris, A.C. Bliton, M.H. Wade, B. Athey, *J. Microsc. (Oxford)* 181 (1996) 253.
- [22] J. Sytsma, J.M. Vroom, C.J. De Grauw, H.C. Gerritsen, *J. Microsc. (Oxford)* 191 (1998) 39.
- [23] R.I. Ghauharali, R. van Driel, G.J. Brakenhoff, *J. Microsc. (Oxford)* 185 (1997) 375.
- [24] M.J. Cole, J. Siegel, S.E.D. Webb, R. Jones, K. Dowling, P.M.W. French, M.J. Lever, L.O.D. Sucharov, M.A.A. Neil, R. Juskaitis, T. Wilson, *Optics Lett.* 25 (2000) 1361.